



Analyzing the Effect of Series and Shunt Facts Controllers on Optimal Power Flow

M. Lakshmi Kantha Reddy¹, M. Ramprasad Reddy², V. C. Veera Reddy³

Research Scholar, Department of Electrical Engineering, SV University, Tirupathi, India^{1&2}

Former Professor, Department of Electrical Engineering, SV University, Tirupathi, India³

ABSTRACT: The management of power systems becoming more difficult than earlier because of increased competition in the existing power systems as they are required to provide greater profit or to provide same service at low cost and thereby increasing the duration of power systems operating close to security limits. So, a new solution to such operational problems will rely on the upgrading of existing transmission corridors by using recent power electronics controllers, known as Flexible Alternating Current Transmission Systems (FACTS) controllers. The power flow through the line can be changed by varying the voltage magnitude at the two ends, the phase angle or the line impedance. In this paper, the power injection model for thyristor controlled series capacitor and static VAR compensator are provided with its incorporation procedure and optimal location identification procedures. The optimal parameters of these controllers and system are identified using the developed gravitational search algorithm. The effectiveness of the proposed methodology is tested on standard IEEE-30 bus test system with supporting numerical and as well as graphical results.

KEYWORDS: Optimal power flow; Gravitational search algorithm; Non-convex fuel cost; TCSC; SVC; Optimal location.

I. INTRODUCTION

With past and current difficulties in building new lines and the significant increase in power transactions associated with competitive electricity markets, there is a need to operate electric utilities closer to their limits. Hence, maintaining system security is more than ever one of the main concerns for market and system operators. In this scenario, the introduction of Flexible AC Transmission Systems (FACTS) has changed the face of power system operation by effective control of power flow, increasing transmission line stability limits and thereby improving the security of transmission systems. In addition to improvement of security of the system, FACTS controllers can minimize the system active power loss which leads to an efficient utilization of existing power systems.

The setting and operation mode of FACTS devices together with the amount of the power dispatched for each plant, can be adequately optimized by the use of customized security constrained optimal power flow programs [1]. In [2], the authors proposed an OPF-based market clearing algorithm that accounted for voltage stability limits. The effect of FACTS devices on the power system security according to proper control objective can enhance the power system security [3]. The security constrained OPF program minimizes the pre-contingency objective function while observing both the pre- and post-contingency system constraints [4]. FACTS devices enhance the static security and reduce the power losses in a given power system [5].

Static security assessment of a power system copes with analyzing the system steady state operation after disturbances. The ordering of insecure contingencies in terms of their severity is known as contingency ranking. The severity of contingencies is assessed based on a performance index (PI). A mere and straight approach to this problem would involve performing full AC load flow for each contingency event followed by operating limit violations has been reported in [6-8]. Various PI-based methods for contingency screening and ranking have been reported in literatures [9-14]. These traditional approaches are hard to put through online due to high computational requirements.

FACTS devices which can control the parameters and variables of the transmission line, i.e. line impedance, terminal voltages, and voltage angles in a fast and effective way. These FACTS devices not only improve the dynamic

International Journal of Advanced Research in Electrical, Electronics and Instrumentation Engineering

(An ISO 3297: 2007 Certified Organization)

Vol. 4, Issue 12, December 2015

behavior more over enhancement of system reliability. However, the main function of FACTS is to control power flows.

In this paper, the detailed analysis of the former literature reveals that incorporation of all the FACTS devices for power flow management in transmission line. But, this paper describes the performance of one of series FACTS device which is TCSC and one of shunt FACTS device which is SVC. In this chapter a method to determine the optimal location of SVC and TCSC is suggested. A mathematical model of TCSC and SVC which is commonly known as power injection model is presented. Power injection model of TCSC and SVC is associated with NR load flow method to study the effects of device parameters and characteristics in power flow studies. The OPF problem is solved with generation non-convex fuel cost as an objective is solved. Numerical analysis is carried out on standard IEEE-30 bus system to demonstrate the performance of the TCSC and SVC.

II. OPERATING PRINCIPLE OF TCSC

TCSC is one of the series compensator; it can capable to control power flow in line, damping power oscillations. Basic simple TCSC model is shown in Fig.1. TCSC is formed by connecting the capacitor in series with the transmission line and thyristor-controlled reactor (TCR) in parallel with capacitor.

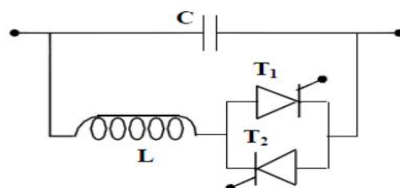


Fig.1 Model of TCSC

A. POWER INJECTION MODEL OF TCSC

The Fig.2 shows a π model of transmission line with TCSC connected between bus-k and bus-m [15]. Under the steady state condition, the TCSC can be represented as a static reactance $-jX_C$. In the power flow equations the controllable reactance X_C is directly used as the control variable.

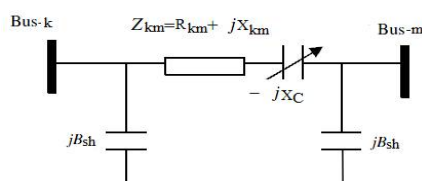


Fig.2 Transmission line with TCSC

The line data will be modified by placing TCSC in series with line. A new line reactance is given as follows

$$X_{km}^{new} = X_{km} - X_C \quad (1)$$

Therefore new line admittance between buses k and m can be derived as follows

$$Y'_{km} = \frac{1}{Z'_{km}} = \frac{1}{R_{km} + j(X_{km} - X_C)} \quad (2)$$

$$Y'_{km} = G'_{km} + jB'_{km} = \frac{R_{km} - j(X_{km} - X_C)}{R_{km}^2 + (X_{km} - X_C)^2} \quad (3)$$

$$G'_{km} = \frac{R_{km}}{R_{km}^2 + (X_{km} - X_C)^2} \quad (4)$$

$$B'_{km} = -\frac{(X_{km} - X_C)}{R_{km}^2 + (X_{km} - X_C)^2} \quad (5)$$

International Journal of Advanced Research in Electrical, Electronics and Instrumentation Engineering

(An ISO 3297: 2007 Certified Organization)

Vol. 4, Issue 12, December 2015

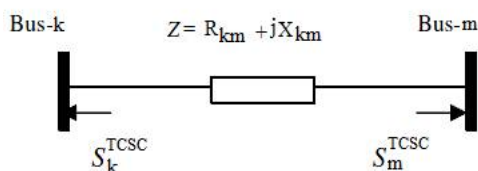


Fig.3 Power injection model of TCSC

Due to TCSC, the change in line flow can be represented as a line without TCSC plus with power injected at the sending and receiving ends of the line with device as shown in Fig.3. The active and reactive power injections at bus-k and bus-m can be written as

$$P_k^{TCSC} = P_{km} - P_{km}^{TCSC} = V_k^2 \Delta G_{km} - V_k V_m [\Delta G_{km} \cos(\delta_{km}) + \Delta B_{km} \sin(\delta_{km})] \quad (6)$$

$$P_m^{TCSC} = P_{mk} - P_{mk}^{TCSC} = V_m^2 \Delta G_{km} - V_k V_m [\Delta G_{km} \cos(\delta_{km}) - \Delta B_{km} \sin(\delta_{km})] \quad (7)$$

$$Q_k^{TCSC} = Q_{km} - Q_{km}^{TCSC} = -V_k^2 \Delta B_{km} - V_k V_m [\Delta G_{km} \sin(\delta_{km}) - \Delta B_{km} \cos(\delta_{km})] \quad (8)$$

$$Q_m^{TCSC} = Q_{mk} - Q_{mk}^{TCSC} = -V_m^2 \Delta B_{km} + V_k V_m [\Delta G_{km} \sin(\delta_{km}) + \Delta B_{km} \cos(\delta_{km})] \quad (9)$$

Where,

$$\Delta G_{km} = \frac{X_C R_{km} (X_C - 2X_{km})}{(R_{km}^2 + X_{km}^2)(R_{km}^2 + (X_{km} - X_C)^2)} \quad (10)$$

$$\Delta B_{km} = \frac{-X_C (R_{km}^2 + X_C X_{km} - X_{km}^2)}{(R_{km}^2 + X_{km}^2)(R_{km}^2 + (X_{km} - X_C)^2)} \quad (11)$$

TCSC device is modeled with power injection model so far by using the TCSC control variable. It is possible to calculate the complex power injected S_k^{TCSC} and S_m^{TCSC} at bus-k and bus-m respectively.

$$S_k^{TCSC} = P_k^{TCSC} + jQ_k^{TCSC} \quad (12)$$

$$S_m^{TCSC} = P_m^{TCSC} + jQ_m^{TCSC} \quad (13)$$

Then new power flow equations can be expressed by the following relationship

$$\begin{bmatrix} \Delta P \\ \Delta Q \end{bmatrix} = \begin{bmatrix} H_{new} & N_{new} \\ J_{new} & L_{new} \end{bmatrix} \begin{bmatrix} \Delta \delta \\ \frac{\Delta V}{V} \end{bmatrix} \quad (14)$$

here new mismatch vectors are

$$\Delta P_i = P_i^{spec} + P_k^{TCSC} - P_k^{calc} \quad (15)$$

$$\Delta Q_i = Q_i^{spec} + Q_k^{TCSC} - Q_k^{calc} \quad (16)$$

Where, P_k^{spec} , Q_k^{spec} are the classical specified real and reactive powers, P_k^{TCSC} , Q_k^{TCSC} are the power injection associated to TCSC devices, P_k^{calc} , Q_k^{calc} are computed using the power flow equations. Now modified Jacobian matrix due to power injections of TCSC

$$H_{new} = H + \frac{\partial P^{TCSC}}{\partial \delta} ; N_{new} = N + \frac{\partial P^{TCSC}}{\partial V} V \quad (17)$$

$$J_{new} = J + \frac{\partial Q^{TCSC}}{\partial \delta} ; L_{new} = L + \frac{\partial Q^{TCSC}}{\partial V} V \quad (18)$$

H , M , N and L are the classic sub-Jacobians

B. INSTALLATION COST OF TCSC

In this chapter device life time is considered for 15 years during the analysis.

The Installation cost (IC) of TCSC [15] is

$$IC_{TCSC} = \frac{C_{TCSC} \times S_{TCSC} \times 1000}{n \times 8760} ; \quad \$/h \quad (19)$$

$$\text{Where, } C_{TCSC} = 0.0015S^2 - 0.7130S + 153.75 ; \quad \$/kVAr \quad (20)$$

$$\text{and } S_{TCSC} = |Q_2| - |Q_1| \quad MVAr \quad (21)$$



International Journal of Advanced Research in Electrical, Electronics and Instrumentation Engineering

(An ISO 3297: 2007 Certified Organization)

Vol. 4, Issue 12, December 2015

Here, Q_1, Q_2 are the reactive power flows in the line without and with TCSC, 'n' is the device life time in years (15 years).

C. DEVICE LIMITS

The following minimum and maximum limits are considered for TCSC reactance.

$$-0.8X_{line} \leq X_{TCSC} \leq 0.2X_{line} \quad p.u.$$

D. SELECTION OF OPTIMAL LOCATION FOR TCSC

The power flows of highest severe contingency are considered as base case. From these flows, the branch with least power flow can be considered as the best location for the TCSC device. Because the transmission line has inductive reactance where as the TCSC is a series controlled device which can provide a capacitive reactance so that the total reactance of the branch which leads to the increase of loadability of the line where the device was located. The objective is, to increase the power transfer capability of the transmission line. The power transfer capability of the transmission line depends on the line reactance as well as bus voltages. Hence the loadability of the line can be increased either by reducing line reactance or increasing voltage profile. In order to reduce the reactance of the transmission line TCSC can be used. The voltage profile can be improved by injecting the reactive power at a particular bus where the voltage is minimum. The optimal location of the device is that where it gives maximum benefit for optimal size of FACTS devices placed at selected location.

i. CONTINGENCY ANALYSIS

Usually, outage of one of the transmission lines can be considered as the contingency condition. This happens due to many reasons; it may be because of maintenance of the transmission lines, environmental conditions, etc. Because of this situation, the transmission lines get overloaded. This contingency analysis analyzes the system security and gives future directions for the proper planning and designing. Because of this analysis, the preventive and corrective measures under contingency conditions can be predicted. Usually, the contingency condition may be due to a transmission line or a generator failure or a transformer failure. Out of which, transmission line failure plays an important role to assess the power system security.

ii. PERFORMANCE INDEX AND RANKING

It is not required to consider each and every line outage to assess power system security. Because, for a particular line outage, there are few lines and buses do not have line flow and voltage variations beyond the limits. If there are any line overloads and bus voltage variations then the outage line is considered as critical line. The critical lines or credible contingencies are identified by contingency analysis and only these critical lines need to be taken to assess the power system security. A parameter which is known as performance index used for security analysis [16]. It indicates how much a particular outage might affect the security of power system. In general the performance index (PI) or severity index (SI) is defined as

$$\text{Severity index} = \sum_{l=1}^{N_{line}} \left(\frac{S_l}{S_l^{max}} \right)^{2m} \quad (22)$$

Where, S_l, S_l^{max} are the MVA flow in line 'l' and MVA rating of the line 'l' respectively. 'm' is an integer exponent taken as 0.5.

The line flows are obtained by using power flow solution method. In Eqn. (22), the performance index is defined only based on over loaded lines.

III. STATIC VAR COMPENSATOR (SVC)

The IEEE definition of the SVC is as follows: "A shunt connected static VAR generator or absorber whose output is adjusted to exchange capacitive or inductive current so as to maintain or control specific parameters of the electrical power system (typically bus voltage)."

SVCs are used in a given power systems to enhance the voltage levels so that system stability has been improved.

International Journal of Advanced Research in Electrical, Electronics and Instrumentation Engineering

(An ISO 3297: 2007 Certified Organization)

Vol. 4, Issue 12, December 2015

A. POWER INJECTION MODEL OF SVC

In practice the SVC can be seen as an adjustable reactance with either firing-angle limits or reactance limits [17]. The equivalent circuit shown in Fig.3.4 is used to derive the SVC nonlinear power equations and the linearized equations required by Newton's method. With reference to Fig.4, the current drawn by the SVC is

$$I_{SVC} = jB_{SVC}V_i \quad (23)$$

and the reactive power drawn by the SVC, which is also the reactive power injected at bus-i, is

$$Q_{SVC} = Q_i = -V_i^2 B_{SVC} \quad (24)$$

It is a bank of three-phase static capacitors and/or inductors. Under heavy loading conditions, when positive VAr is needed, capacitor banks are needed, when negative VAr is needed, inductor banks are used. In this thesis SVC is modeled as an ideal reactive power injection at bus-i shown in Fig.4.

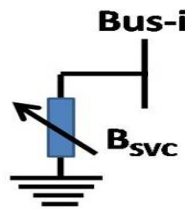


Fig.4. Power injection model of SVC

B. INSTALLATION COST OF SVC

The Installation Cost (IC) [17] of SVC can be expressed as

$$IC_{SVC} = \frac{C_{SVC} \times S_{SVC} \times 1000}{n \times 8760} ; \quad \$/h \quad (25)$$

Here, Cost of Installation of SVC is

$$C_{SVC} = 0.0003S_{SVC}^2 - 0.3051S_{SVC} + 127.38 ; \quad \$/kVAr$$

Operating range of SVC (S_{SVC}) in MVar is $S_{SVC} = |Q_{SVC}|$

Where, Q_{SVC} is the reactive power injected by SVC.

C. DEVICE LIMITS

The following limits are considered for SVC

$$-100 \text{ MVar} \leq Q_{SVC} \leq 100 \text{ MVar}$$

D. SELECTION OF OPTIMAL LOCATION FOR SVC

The SVC should be placed in an optimal location to enhance the system stability.

i. VOLTAGE STABILITY INDEX

The voltage stability index or L -index gives literally consistent results for voltage collapse prediction compared to other methods [18]. The L -indices are computed for all the load buses. The L -index gives a scalar integer to each load bus. The maximum of the L -indices gives the proximity of the system to voltage collapse. The benefit of this method is the simplicity of the numerical calculation and clarity of the results. For the given operating conditions, the voltage stability index is computed using load flow results and is given by

$$L_j = \left| 1 - \sum_{i=1}^{NG} F_{ij} \frac{V_i}{V_j} \right| \quad (26)$$

Where, $j = NG + 1, \dots, NB$, V_i and V_j are the complex voltages of i^{th} and j^{th} bus respectively, F_{ji} are the complex elements of the matrix $[F_{LG}]$.

The matrix $[F_{LG}]$ is obtained from the bus admittance matrix $[Y_{bus}]$.

If the L -index values for load buses are close to zero, indicates the system has maximum stability margin. If it is close to one, indicates the system is close to voltage collapse.

The following procedure is used to identify suitable SVC location and incorporation procedure.

Step1: Perform Newton Raphson load flow on a given system.

Step2: Obtain the system bus voltage magnitude values.

Step3: Calculate the Voltage Stability Index (VSI) at load buses.



International Journal of Advanced Research in Electrical, Electronics and Instrumentation Engineering

(An ISO 3297: 2007 Certified Organization)

Vol. 4, Issue 12, December 2015

Step4: Place the SVC at the bus, where the VSI value is high when compared to other buses.
Step5: In this location, with SVC, the VSI value has been enhanced.

IV. OPF PROBLEM FORMULATION

The aim of optimal power flow solution is, to optimize the selective objective function through proper adjustment of control variables by satisfying various constraints. The OPF problem can be represented as follows:

$$\text{Min } [A_m(x, u)] \quad (27)$$

Subjected to $g(x, u) = 0$ and $h_{min} \leq h(x, u) \leq h_{max}$

Where,

$A_m(x, u)$ is the function which is to be minimized

$g(x, u), h(x, u)$ represents equality and inequality constraints

'x' and 'u' are dependent and independent variables

Optimal power flow solution gives an optimal control variable leads to the minimum generation fuel cost, emission and total power loss etc. subjected to all the various equality and inequality constraints. Here the vector 'x' consists of slack bus real power output (P_{G1}), generator VAR output (Q_G), load bus voltage magnitude (V_L), line flow limits (S_l)

Thus 'x' can be written as,

$$x^T = [P_{G1}, V_{L1}, \dots, V_{LNL}, Q_{G1}, \dots, Q_{GNG}, S_{l1}, \dots, S_{lnl}] \quad (28)$$

Where,

NL=Number of load buses

NG=Number of generator buses

nl=Number of lines

u=is the independent variable vector such as continuous and discrete variables consists of

- (i) Generator active output 'P_G' at all generators without slack bus
- (ii) Generator voltages V_G
- (iii) Tap settings of transformer 'T'
- (iv) Shunt VAR compensation(or) reactive power injections Q_C

Here P_G, V_G are continuous variables and T and Q_C are the discrete variables. Hence 'u' can be expressed as

$$u^T = [P_{G2}, \dots, P_{GNG}, V_{G1}, \dots, V_{GNG}, Q_{C1}, \dots, Q_{Cnc}, T_1, \dots, T_{NT}] \quad (29)$$

'NT' and 'nc' re number of tap controlling transformers and shunt compensators.

A. NON-CONVEX FUEL COST

In general, the generating units are supplied with multiple valves for the steam turbines. Because of the valve-point, the ripples and the non-linearities present in the operation of the generating units. Because of this valve-point effect the generating units shows non-convex, non-smooth input-output characteristics. The conventional fuel cost function can be modified as the non-convex fuel cost function and can be expressed as follows.

$$C_i(P_{G_i}) = a_i P_{G_i}^2 + b_i P_{G_i} + c_i + |e_i \times \sin(f_i \times (P_{G_i}^{min} - P_{G_i}))| \quad (30)$$

Where, a_i, b_i, c_i are the fuel cost coefficients of i^{th} unit, P_{G_i} is the active power generation of i^{th} unit. e_i and f_i are the fuel cost-coefficients of the i^{th} unit reflecting valve-point loading effects.

Total fuel cost objective function is formulated by combining FACTS investment cost (IC_{FACTS}) along with the conventional fuel cost function. Because of the combining FACTS cost with fuel cost function, the system and the FACTS controller control variables are readjusted to optimize the combined fuel cost function. This objective function is optimized while satisfying system operating, practical and the device limits. The modified fuel cost function with device investment cost can be expressed as follows:

$$\text{Quadratic fuel cost with TCSC} \quad A_{cost} = \sum_{i=1}^{NG} C_i(P_{G_i}) + IC_{TCSC} \quad (31)$$



International Journal of Advanced Research in Electrical, Electronics and Instrumentation Engineering

(An ISO 3297: 2007 Certified Organization)

Vol. 4, Issue 12, December 2015

$$\text{Quadratic fuel cost with SVC} \quad A_{cost} = \sum_{i=1}^{NG} C_i(P_{G_i}) + IC_{SVC} \quad (32)$$

$$\text{Quadratic fuel cost with TCSC & SVC} \quad A_{cost} = \sum_{i=1}^{NG} C_i(P_{G_i}) + IC_{TCSC} + IC_{SVC} \quad (33)$$

Where, ' A_{cost} ' is the total generation cost, ' $C_i(P_{G_i})$ ' is the fuel cost function of the i^{th} unit, ' P_{G_i} ' is the power generated by the i^{th} unit and 'NG' is the total number of generating units.

B. CONSTRAINTS

Constraints made in this OPF problem are usually two types. They are equality constraints and inequality constraints.

i. EQUALITY CONSTRAINTS

These constraints mentioned in Eqn. (29) are usually load flow equations described as

$$P_{g,k} - P_{d,k} - \sum_{m=1}^{N_{bus}} |V_k| |V_m| |Y_{km}| \cos(\theta_{km} - \delta_k + \delta_m) = 0 \quad (34)$$

$$Q_{G,k} - Q_{d,k} - \sum_{m=1}^{N_{bus}} |V_k| |V_m| |Y_{km}| \sin(\theta_{km} - \delta_k + \delta_m) = 0 \quad (35)$$

where $P_{G,k}$, $Q_{G,k}$ are the active and reactive power generation at the k^{th} bus, $P_{d,k}$, $Q_{d,k}$ are the active and reactive power demands at the k^{th} bus, $|V_k|$, $|V_m|$ are the voltage magnitudes at the k^{th} and m^{th} buses, δ_k , δ_m are the phase angles of the voltage at the k^{th} and m^{th} buses, and $|Y_{km}|$, θ_{km} are the bus admittance magnitude and its angle between the k^{th} and m^{th} buses.

ii. INEQUALITY CONSTRAINTS

These are the constraints represents the system operational and security limits which are continuous and discrete constraints.

Generator bus voltage limits:	$V_{G_i}^{min} \leq V_{G_i} \leq V_{G_i}^{max} \quad \forall i \in NG$
Active power generation limits:	$P_{G_i}^{min} \leq P_{G_i} \leq P_{G_i}^{max} \quad \forall i \in NG$
Transformers tap setting limits:	$T_i^{min} \leq T_i \leq T_i^{max} \quad \forall i \in nt$
Capacitor reactive power generation limits:	$Q_{sh_i}^{min} \leq Q_{sh_i} \leq Q_{sh_i}^{max} \quad \forall i \in nc$
Transmission line flow limit:	$S_{l_i} \leq S_{l_i}^{max} \quad \forall i \in nl$
Reactive power generation limits:	$Q_{G_i}^{min} \leq Q_{G_i} \leq Q_{G_i}^{max} \quad \forall i \in NG$
Load bus voltage magnitude limits:	$V_i^{min} \leq V_i \leq V_i^{max} \quad \forall i \in NL$

The control variables in this problem are self-constrained, whereas the in-equality constraints such as P_{G_i} , V_i , Q_{G_i} , and S_{l_i} are non-self-constrained by nature. Hence, these inequalities are incorporated into the objective function using a penalty approach [19]. The augmented function can be formulated as:

$$A_{aug}(x, u) = A(x, u) + R_1 (P_{G_1} - P_{G_1}^{lim})^2 + R_2 \sum_{i=1}^{NL} (V_i - V_i^{lim})^2 + R_3 \sum_{i=1}^{NG} (Q_{G_i} - Q_{G_i}^{lim})^2 + R_4 \sum_{i=1}^{nl} (S_{l_i} - S_{l_i}^{max})^2 \quad (36)$$

where R_1 , R_2 , R_3 , and R_4 are the penalty quotients, which take large positive values. The limit values of the dependent variable x^{lim} can be given as:

$$x^{lim} = \begin{cases} x, & x^{min} \leq x \leq x^{max} \\ x^{max}, & x \geq x^{max} \\ x^{min}, & x \leq x^{min} \end{cases}$$

Where, ' x^{lim} ' can be P_{G_1} , V_i , Q_{G_i} .



International Journal of Advanced Research in Electrical, Electronics and Instrumentation Engineering

(An ISO 3297: 2007 Certified Organization)

Vol. 4, Issue 12, December 2015

V. GRAVITATIONAL SEARCH ALGORITHM

In this section, the developed optimization algorithm based on the law of gravity. In the proposed algorithm, agents are considered as objects and their performance is measured by their masses. All these objects attract each other by the gravity force, and this force causes a global movement of all objects towards the objects with heavier masses. Hence, masses cooperate using a direct form of communication, through gravitational force. The heavy masses – which correspond to good solutions – move more slowly than lighter ones, this guarantees the exploitation step of the algorithm.

In GSA, each mass (agent) has four specifications: position, inertial mass, active gravitational mass, and passive gravitational mass. The position of the mass corresponds to a solution of the problem, and its gravitational and inertial masses are determined using a fitness function.

In other words, each mass presents a solution, and the algorithm is navigated by properly adjusting the gravitational and inertia masses. By lapse of time, we expect that masses be attracted by the heaviest mass. This mass will present an optimum solution in the search space.

The GSA could be considered as an isolated system of masses. It is like a small artificial world of masses obeying the Newtonian laws of gravitation and motion. More precisely, masses obey the following laws:

Law of gravity: Each particle attracts every other particle and the gravitational force between two particles is directly proportional to the product of their masses and inversely proportional to the distance between them, R. We use here R instead of R^2 because according to our experiment results, R provides better results than R^2 in all experimental cases.

Law of motion: The current velocity of any mass is equal to the sum of the fraction of its previous velocity and the variation in the velocity. Variation in the velocity or acceleration of any mass is equal to the force acted on the system divided by mass of inertia.

The gravitational constant, G, is initialized at the beginning and will be reduced with time to control the search accuracy. In other words, G is a function of the initial value (G_0) and time (t):

$$G(t) = G(0) \times \exp\left(\frac{-\alpha t_i}{T}\right) \quad (37)$$

Where, α is a constant, t_i is the iteration number and 'T' is the total number of iterations.

Consider a system of N agents. The position of i^{th} agent is defined as

$$X_i = (x_i^1, \dots, x_i^d, \dots, x_i^n) \quad ; \quad i = 1, 2, 3, \dots, N \quad (38)$$

For each position fitness function is evaluated.

VI. MATHEMATICAL CALCULATIONS

The parameters are calculated as per the following calculations.

A. CALCULATION OF MASSES

Let $fit_i(t)$ be the fitness function of i^{th} particle at t^{th} iteration.

Now we introduce new variables $worst(t)$ and $best(t)$.

For a minimization problem, $worst(t)$ and $best(t)$ are defined as follows:

$$best(t) = \min(fit_j(t)) \quad ; \quad j = 1, 2, \dots, N \quad (39a)$$

$$worst(t) = \max(fit_j(t)) \quad ; \quad j = 1, 2, \dots, N \quad (39b)$$

For a maximization problem, $worst(t)$ and $best(t)$ are defined as follows:

$$best(t) = \max(fit_j(t)) \quad ; \quad j = 1, 2, \dots, N \quad (40a)$$

$$worst(t) = \min(fit_j(t)) \quad ; \quad j = 1, 2, \dots, N \quad (40b)$$

Gravitational and inertia masses are simply calculated by the fitness evaluation. A heavier mass means a more efficient agent. This means that better agents have higher attractions and walk more slowly. Assuming the equality of the gravitational and inertia mass, the values of masses are calculated using the map of fitness. We update the gravitational and inertial masses by the following equations:

$$M_{ai} = M_{pi} = M_{ii} = M_i \quad (41a)$$



International Journal of Advanced Research in Electrical, Electronics and Instrumentation Engineering

(An ISO 3297: 2007 Certified Organization)

Vol. 4, Issue 12, December 2015

$$m_i(t) = \frac{fit_i(t) - worst(t)}{best(t) - worst(t)} \quad (41b)$$

$$M_i(t) = \frac{m_i(t)}{\sum_{j=1}^N m_j(t)} \quad (41c)$$

B. CALCULATION OF FORCE

For iteration t , we define the force acting on mass i from mass j as following.

$$F_{ij}^d(t) = G(t) \frac{M_{pi}(t)M_{aj}(t)}{R_{ij} + \epsilon} (x_j^d - x_i^d) \quad (42)$$

Where, M_{aj} , M_{pi} are the active and passive gravitational masses related to agent j , $G(t)$ is gravitational constant at iteration t , ϵ is a small constant and R_{ij} is the Euclidian distance between two agents i and j given by

$$R_{ij}(t) = \|X_i(t) - X_j(t)\|_2 \quad (43)$$

To give a stochastic characteristic to our algorithm, we suppose that the total force that acts on agent i in a dimension d be a randomly weighted sum of d^{th} components of the forces exerted from other agents:

$$F_i^d(t) = \sum_{j=1, j \neq i}^N rand_i F_{ij}^d(t) \quad (44)$$

One way to perform a good compromise between exploration and exploitation is to reduce the number of agents with lapse of time. Hence, we propose only a set of agents with bigger mass apply their force to the other. However, we should be careful of using this policy because it may reduce the exploration power and increase the exploitation capability.

We remind that in order to avoid trapping in a local optimum the algorithm must use the exploration at beginning. By lapse of iterations, exploration must fade out and exploitation must fade in. To improve the performance of GSA by controlling exploration and exploitation only the K_{best} agents will attract the others. K_{best} is a function of time, with the initial value K_0 at the beginning and decreasing with time. In such a way, at the beginning, all agents apply the force, and as time passes, K_{best} is decreased linearly and at the end there will be just one agent applying force to the others.

Therefore, could be modified as:

$$F_i^d(t) = \sum_{j=K_{best}, j \neq i}^N rand_i F_{ij}^d(t) \quad (45)$$

Where K_{best} is the set of first K agents with the best fitness value and biggest mass given by

$$k_{best} = final_{per} + \left(1 - \frac{t}{T}\right) (100 - final_{per}) \quad (46)$$

Where, $final_{per}$ is the percentage of particles remains at the end (generally 2). Since M is a function of m , which is function fitness, in every iteration, one value of m is zero. Hence M is zero at this value of m . At this value of M acceleration becomes an indefinite value from above equations. To obtain integer value of K_{best} , it is rounded in terms of population. Hence we introduce another variable E which is defined as follows:

$$E_{ij}^d = \frac{F_{ij}^d}{MG} = \frac{M}{R_{ij} + \epsilon} (x_j^d - x_i^d) \quad (47)$$

$$E_i^d(t) = \sum_{j=1, j \neq i}^N rand_i E_{ij}^d(t) \quad (48)$$

C. CALCULATION OF ACCELERATION

Hence, by the law of motion, the acceleration of the agent ' i ' at iteration t , and in direction d , is given as:

$$a_i^d = E_i^d(t) \times G(t) \quad (49)$$

Furthermore, the next velocity of an agent is considered as a fraction of its current velocity added to its acceleration. Therefore, its position and its velocity could be calculated as follows:

$$V_i^d(t+1) = rand_i \times V_i^d(t) + a_i^d(t) \quad (50a)$$

$$x_i^d(t+1) = x_i^d(t) + V_i^d(t+1) \quad (50b)$$

International Journal of Advanced Research in Electrical, Electronics and Instrumentation Engineering

(An ISO 3297: 2007 Certified Organization)

Vol. 4, Issue 12, December 2015

D. STEP BY STEP PROCEDURE OF GSA

The different steps of the proposed algorithm are the followings:

- i). Search space identification.
- ii). Randomized initialization.
- iii). Fitness evaluation of agents.
- iv). Update $G(t)$, $best(t)$, $worst(t)$ and $M_i(t)$ for $i = 1, 2, \dots, N$.
- v). Calculation of the total force in different directions.
- vi). Calculation of acceleration and velocity.
- vii). Updating agents' position.
- viii). Repeat steps iii to vii until the stop criteria is reached.
- ix). End.

E. FLOW CHART OF GSA

The complete procedure of GSA is shown in flow chart Figure.5.

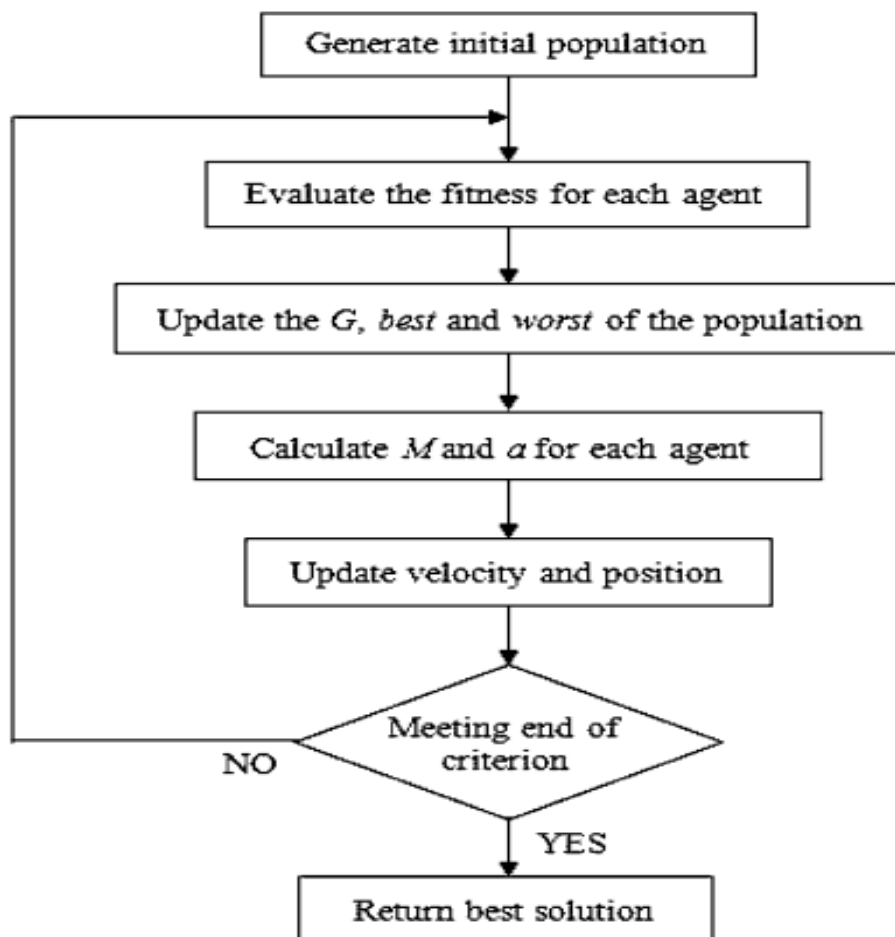


Fig.5 Flow chart of GSA



International Journal of Advanced Research in Electrical, Electronics and Instrumentation Engineering

(An ISO 3297: 2007 Certified Organization)

Vol. 4, Issue 12, December 2015

VII. RESULTS AND ANALYSIS

In order to demonstrate the effectiveness and robustness of the proposed GSA method with TCSC and SVC, IEEE 30 bus system is considered. The existing and proposed methodologies are implemented on a personal computer with Intel Core2 Duo 1.18 GHz processor and 2 GB RAM. The input parameters of existing PSO method and the proposed GSA method for the considered test system are given in Table.1.

Table.1 Input parameters for test system

S. No	Optimization Method	Parameters	Quantity
1	PSO method	Population size	5
		Number of generations	100
		Initial weight function, ω_{max}	0.9
		Final weight function, ω_{min}	0.4
		Acceleration coefficients c_1 and c_2	2
2	GSA method	Population	50
		Maximum iterations	100
		Initial gravitational constant (G_0)	100
		Decay constant (α)	5/10
		Constant (ϵ)	8.854×10^{-12}
		Percentage of number of particles in final iteration	2
		Rnorm	2

This section presents the details of the study carried out on IEEE-30 bus test system to analyze OPF problem. The network and load data for this system is taken from [20]. In the IEEE 30-bus system consist 41 branches, six generator buses and 21 load buses. Four branches 6-9, 6-10, 4-12 and 27-28 have tap changing transformers.

The buses with possible reactive power source installations are 10 and 24. As the SVC is a shunt controlled FACTS device, the bus which suffers from high voltage stability index is required to install SVC. The VSI values at load buses are given in Table.2.

Table.2. Load bus VSI values for IEEE-30 bus system

S. No.	Bus Number	VSI value
1	3	0.01318
2	4	0.01437
3	6	0.01268
4	7	0.01984
5	9	0.03657
6	10	0.07079
7	12	0.04427
8	14	0.06569
9	15	0.07047
10	16	0.06234
11	17	0.07342
12	18	0.08704
13	19	0.09232
14	20	0.08797
15	21	0.08226
16	22	0.08185
17	23	0.08409
18	24	0.09293
19	25	0.0927
20	26	0.10803
21	27	0.08475
22	28	0.0179
23	29	0.11342
24	30	0.13311

International Journal of Advanced Research in Electrical, Electronics and Instrumentation Engineering

(An ISO 3297: 2007 Certified Organization)

Vol. 4, Issue 12, December 2015

From the above table, it is identified that, bus-30 has the highest VSI value and is suitable to install SVC, because of this the VSI value has been enhanced. The respective variation of VSI values at load buses is shown in Fig.6.

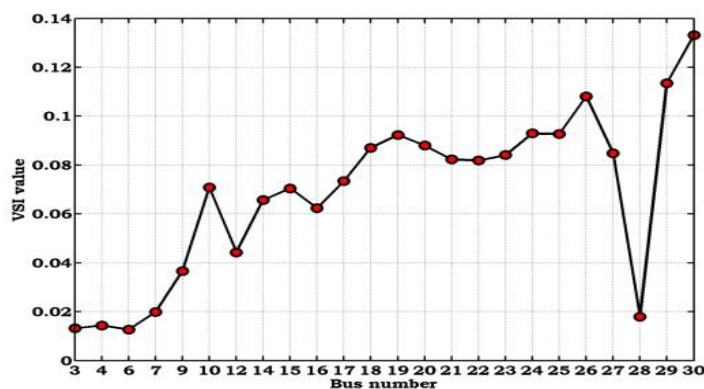


Fig.6 Variation of VSI values for IEEE-30 bus system

From the base case analysis and from the power flows given in Table.3, it is observed that, the best location to install TCSC is between buses 29 and 30 i.e. line-39. For this line, the actual thermal limits is 16 MVA but at the actual flow is 3.753 MVA, there is a margin of 12.247 MVA for which we can increase the power flow.

Table.3 Power flows under base case for IEEE-30 bus system

Line No	From Bus	To bus	Line Flow(MVA)	Line Limit (MVA)
1	1	2	120.4917	130
2	1	3	58.0031	130
3	2	4	33.2879	65
4	3	4	54.0435	130
5	2	5	58.7088	130
6	2	6	44.5083	65
7	4	6	50.1597	90
8	5	7	10.064	70
9	6	7	30.3389	130
10	6	8	16.514	32
11	6	9	19.8451	65
12	6	10	12.4788	32
13	9	11	18.1698	65
14	9	10	29.2026	65
15	4	12	31.6852	65
16	12	13	21.4605	65
17	12	14	8.6429	32
18	12	15	20.8947	32
19	12	16	9.6173	32
20	14	15	2.1168	16
21	16	17	5.6389	16
22	15	18	7.1659	16
23	18	19	3.7849	16
24	19	20	6.438	32
25	10	20	8.8739	32



International Journal of Advanced Research in Electrical, Electronics and Instrumentation Engineering

(An ISO 3297: 2007 Certified Organization)

Vol. 4, Issue 12, December 2015

26	10	17	5.8884	32
27	10	21	18.6425	32
28	10	22	8.8685	32
29	21	22	2.3894	32
30	15	23	6.9155	16
31	22	24	6.449	16
32	23	24	3.2819	16
33	24	25	1.3101	16
34	25	26	4.2621	16
35	25	27	3.5338	16
36	28	27	17.5636	65
37	27	29	6.411	16
38	27	30	7.2844	16
39	29	30	3.753	16
40	8	28	2.4462	32
41	6	28	15.6361	32

From the above analysis, the optimal location to install SVC is bus 30 and for TCSC is line-30 between buses 29 and 30. The further analysis is assumed by placing these devices in these locations.

In this, the results of optimized values for all control variables for minimization of non-convex cost objective with proposed GSA method. The summary of test results with TCSC and SVC are given in Table.4 and it is observed that the non-convex fuel cost is reduced by 0.6963 \$/h with TCSC, 2.2745 \$/h with SVC and 2.5771 \$/h with both devices when compared to without device. Similarly, the respective losses with all devices are also tabulated.

Table.4. OPF results of non-convex cost with SVC and TCSC for IEEE-30 bus system

S. No	Control Parameters	Without Device	With			
			TCSC	SVC	TCSC& SVC	
1	Real power Generation (MW)	P_{G1}	191.8449	193.8541	193.5638	192.9128
		P_{G2}	41.41166	44.69628	43.73358	41.86696
		P_{G5}	19.44287	20.63099	18.6279	19.91949
		P_{G8}	18.95174	12.33587	15.53649	16.54543
		P_{G11}	10.1208	10.7479	10.23062	10.13091
		P_{G13}	12	12	12	12
2	Generator voltages (p.u.)	V_{G1}	1.087533	1.067232	1.1	1.1
		V_{G2}	1.066829	1.045436	1.03549	1.078088
		V_{G5}	1.035831	1.027194	1.064572	1.05409
		V_{G8}	1.051681	1.036143	1.079418	1.062661
		V_{G11}	1.059621	1.038693	1.005867	1.035137
		V_{G13}	0.965	1.044286	1.024848	1.016772
3	Transformer tap setting (p.u.)	T_{6-9}	1.064279	1.013001	1.071545	1.098525
		T_{6-10}	1.012959	0.944851	1.073251	1.066475
		T_{4-12}	0.900387	1.01988	1.063123	1.059689
		T_{28-27}	1.010379	1.038715	1.012484	1.042249
4	Shunt compensators (MVar)	$Q_{C,10}$	13.00939	15.25366	17.54817	14.56866
		$Q_{C,24}$	27.3251	25.60134	9.908207	20.72563
5	X_{TCSC} , p.u.	-	0.04306	-	-0.54648	
6	Q_{SVC} , p.u.	-	-	0.161653	0.09982	
7	Total generation (MW)	293.7719	294.2652	293.6924	293.3756	
8	Non-convex fuel cost (\$/h)	919.0168	918.3205	916.7423	916.4397	
9	Total power losses (MW)	10.37194	10.86518	10.29237	9.975577	

International Journal of Advanced Research in Electrical, Electronics and Instrumentation Engineering

(An ISO 3297: 2007 Certified Organization)

Vol. 4, Issue 12, December 2015

The convergence characteristics of the proposed algorithm for all the cases are shown in Fig.7 and it is observed that, in the presence of both devices, the iterative process starts with good function value and reached final best value in more number of iterations when compared to without and with TCSC and SVC. This is because of solving OPF in the presence of devices.

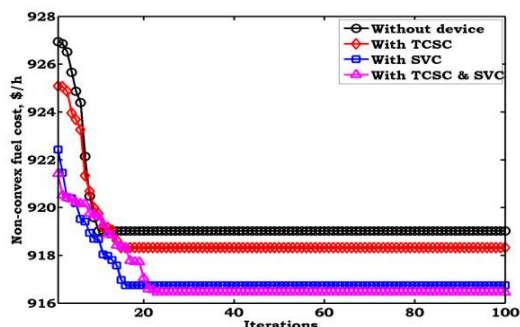


Fig.7. Convergence characteristics of non-convex fuel cost with SVC and TCSC for IEEE-30 bus system

The voltage magnitude at buses and power flow in transmission lines are tabulated in Tables.5 and 6.

Table.5 Voltage magnitudes of non-convex fuel cost with SVC and TCSC for IEEE-30 bus system

Bus No	Without device	With		
		TCSC	SVC	TCSC & SVC
1	1.0875329	1.0672323	1.1	1.1
2	1.066829	1.0454359	1.07532283	1.0780879
3	1.0488611	1.041824	1.0760524	1.0723877
4	1.0396648	1.0354867	1.06990093	1.0654657
5	1.035831	1.0271936	1.06457235	1.0540897
6	1.0471897	1.03184	1.06941615	1.0627724
7	1.0350538	1.0223166	1.06018197	1.0518835
8	1.0626608	1.0781529	1.03614285	1.0516808
9	0.9976376	0.9982404	1.03071813	1.028138
10	0.9949036	0.9954162	1.03402061	1.0357508
11	1.0351372	1.005867	1.03869264	1.0596209
12	1.0000466	1.0032987	1.0263071	1.0639722
13	1.0167716	1.024848	1.04428576	1.0437303
14	0.9875959	0.9897917	1.0156023	1.0499289
15	0.9855917	0.9869283	1.01485286	1.0454751
16	0.9902374	0.9923601	1.02213375	1.0447945
17	0.987881	0.9888903	1.02500388	1.0331189
18	0.9760775	0.9771349	1.009241	1.0299237
19	0.9737439	0.9746333	1.00911275	1.0238337
20	0.9782076	0.9790029	1.01453826	1.0260375
21	0.9866779	0.9856788	1.02509383	1.0299071
22	0.9887405	0.9872691	1.02675475	1.0325272
23	0.9861203	0.9837747	1.01717307	1.0426908
24	0.9957352	0.9884088	1.02896357	1.0474619
25	0.991576	1.0029296	1.00439072	1.0323856
26	0.9734207	0.9849882	0.98647645	1.0149758
27	0.9977429	1.0206648	0.99774149	1.0313903
28	1.05935	1.0662622	1.03219929	1.046548
29	0.9763665	1.0041329	0.9774077	1.0117248
30	0.963496	0.9901982	0.96540756	1.0003498



International Journal of Advanced Research in Electrical, Electronics and Instrumentation Engineering

(An ISO 3297: 2007 Certified Organization)

Vol. 4, Issue 12, December 2015

Table.6 Power flows of non-convex fuel cost with SVC and TCSC for IEEE-30 bus system

Line No	Without Device	With			MVA Limit
		TCSC	SVC	TCSC & SVC	
1	129.72062	129.98318	130.06663	129.96273	130
2	62.676047	63.881141	63.580235	62.971618	130
3	35.482794	36.577984	36.53183	35.424483	65
4	58.479343	59.946656	59.751477	59.071727	130
5	64.906624	65.741618	66.839235	65.092596	130
6	46.694899	49.194169	49.242862	47.726074	65
7	59.070078	56.402109	56.936513	54.70456	90
8	12.429914	12.200081	13.299308	12.136396	70
9	35.01526	32.978503	34.224932	34.151859	130
10	20.200542	24.732648	32.066032	16.028732	32
11	27.261412	21.322228	19.411333	24.100922	65
12	12.644106	19.056115	13.090298	13.589651	32
13	18.481587	11.413092	10.829614	20.552983	65
14	28.794789	31.451068	29.796314	30.166714	65
15	55.356197	31.268768	31.375137	31.695705	65
16	19.581916	17.754857	19.480027	16.863335	65
17	8.4627118	7.5554198	7.8011614	7.714001	32
18	20.382717	17.789529	17.897069	17.894586	32
19	10.625902	6.6655132	7.3409381	7.1505419	32
20	1.9679646	1.6024049	1.3425409	1.4204654	16
21	6.5573527	4.1608701	3.4580666	3.4129431	16
22	7.9724355	5.3890587	6.1000114	5.9725717	16
23	4.7188563	2.3639937	2.7178458	2.5951039	16
24	5.9612556	8.5464904	7.4107962	7.5401119	32
25	8.3092974	11.060599	9.909392	10.044621	32
26	4.3419279	10.594933	7.8756604	8.3105576	32
27	15.376534	17.250187	16.202428	15.948482	32
28	7.3925739	8.2017114	7.3878205	7.4132869	32
29	10.573559	6.7980659	5.9618388	7.8759449	32
30	6.5911141	6.4291587	4.5499083	5.5529454	16
31	12.721398	9.1010564	5.7186834	8.8636175	16
32	4.5878989	5.7568066	2.6376752	4.6087458	16
33	5.3107403	7.5651175	3.974014	3.0558028	16
34	4.2599159	4.2641332	4.2643636	4.2661903	16
35	5.1807358	6.0540827	8.2724339	5.4862918	16
36	17.744443	16.735931	21.978144	19.606702	65
37	6.4080197	6.3396442	4.9754588	6.4883107	16
38	7.2807649	7.3818367	8.6193855	7.3829473	16
39	3.7521386	3.672334	2.3376268	3.8004672	16
40	2.0319771	1.048197	3.8667802	2.2629968	32
41	16.18306	16.872205	17.877928	16.998269	32

The variation of voltage magnitude at system buses and the power flow through the transmission lines are shown in Figs. 8 and 9. From these figures, the voltage profile and transmission line loadings are enhanced in the presence of both of the devices instead of single device.

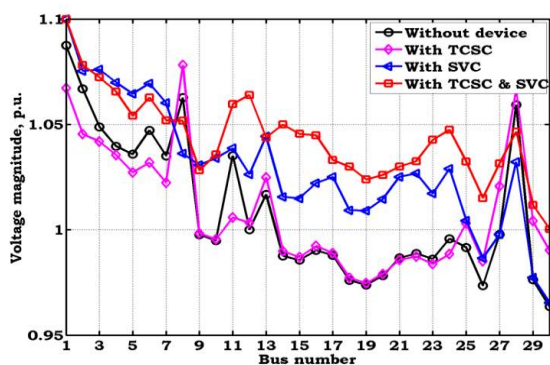


Fig.8. Variation of voltage magnitudes of non-convex fuel cost with SVC and TCSC for IEEE-30 bus system

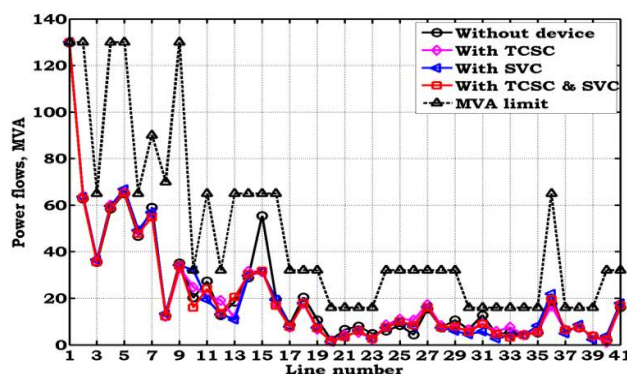


Fig.9. Variation of power flows of non-convex fuel cost with SVC and TCSC for IEEE-30 bus system

To support the effectiveness of the proposed method, obtained results are compared with the existing literature methods. The comparison is given in Table.7. From this table, it is identified that, the proposed method yields good results when compared to existing methods.

Table.7. Validation of SCOPF results of quadratic cost for IEEE-30 bus system

S.No	Method	Quadratic cost (\$/h)
1	EP [21]	802.9070
2	TS/SA [22]	802.7880
3	ITS [23]	804.5560
4	GA [24]	803.0500
5	Proposed GSA	802.7499

From the above analysis, it has been concluded that, because of including security constraints in SCOPF problem, this problem is more efficient when compared to OPF problem. From this, it is assumed that, the further analysis is performed using SCOPF only.

VIII. CONCLUSION

In this paper, the OPF problem with new cost objective formulated by combining non convex fuel cost and investment costs of TCSC and SVC is solved in the presence of TCSC and SVC while satisfying system, constraints and device limits. The effect of these FACTS controllers on bus voltage magnitudes and line power flows has been analyzed. The OPF results obtained in the presence of both TCSC and SVC are compared with that of the results



International Journal of Advanced Research in Electrical, Electronics and Instrumentation Engineering

(An ISO 3297: 2007 Certified Organization)

Vol. 4, Issue 12, December 2015

obtained in the presence of individual controllers. The proposed methodology has been tested on standard IEEE-30 bus test system.

REFERENCES

- [1]. Lehmkoester, C, "Security constrained optimal power flow for an economical operation of FACTS-devices in liberalized energy markets", Power Delivery, IEEE Transactions on, 2002, Vol.17, No.2, pp.603–608.
- [2]. Milano, F. Canizares, C.A. Conejo, A.J., "Sensitivity-Based Security-Constrained OPF Market Clearing Model", Power Systems Conference and Exposition, 2006. PSCE '06. 2006 IEEE PES, Oct. 29-Nov, Vol.1, pp.418-427.
- [3]. M.Noroozian, L. Angquist, M.Ghandhari, Ghderson, "Use of UPFC for Optimal Power Flow Control", IEEE Trans. on Power Delivery, Vol.12, No.4, October 1997.
- [4]. Saleh Aboreshaid, "Impact of Unified Power Flow Controllers on Power System Reliability", IEEE Trum. on Paver Systems Vol. 15, No. 1, February 2000.
- [5]. Momoh, J.A. Zhu, J.Z. Boswell, G.D. Hoffman, S., "Power system security enhancement by OPF with phase shifter", Power Systems, IEEE Transactions on 2001, Vol.16, No.2, pp. 287 – 293.
- [6]. B.Scott and O.Alsac, "Fast Decoupled Load Flow", IEEE Trans on PAS, May 1974, vol. PAS-93. pp. 859-869.
- [7]. H.Mori, H.Tanaka and J.Kanno, "A Preconditioned Fast Decoupled Power Flow method for contingency screening," IEEE Trans. on Power Systems, Feb. 1996, Vol.11, No.1, pp. 357-362.
- [8]. V.Brandwajn and M.J.Lauby, "Complete bounding method for AC contingency screening," IEEE Trans. on Power Systems, May 1989, vol.4, No.2, pp. 724-729.
- [9]. Y. Chen and A. Bose, "Direct ranking for voltage contingency selection," IEEE Trans. on Power Systems, Oct. 1989, Vol. 4, No.4, pp. 1335-1344.
- [10]. M.Pandit, L.Srivastava and J.Sharma, "Fast voltage contingency selection using Fuzzy parallel self-organizing hierarchical neural network," IEEE Trans. on Power Systems, May 2003 Vol.18, No.2, pp. 657-664.
- [10]. Saleh Aboreshaid and Roy Billinton, "Probabilistic evaluation of voltage stability," IEEE Trans. on Power Systems, Feb 1999, vol.14, No.1, pp. 342- 348.
- [12]. Ismail Musirin and Titik Khawa Abdul Rahman, "On-Line voltage stability based contingency ranking using Fast voltage stability index", Transmission and Distribution Conference and Exhibition 2002: Asia Pacific. IEEE/PES, Oct 2002. (Date 6-10), Vol.2, pp. 1118-1123.
- [13]. Ismail Musirin and Titik Khawa Abdul Rahman, "Fast automatic contingency analysis and ranking technique for power system security assessment," IEEE (SCORED) Proceedings, Putrajaya, Malaysia, Aug 2003. (Date 25-26), Vol.1, pp. 231-236.
- [14]. R.H.Chen, J. Gao, O.P.Malik, Wang and Xiang, "Automatic contingency analysis and classification," IEE Power System control and management conference publication April 1996, No.421, pp.16-18.
- [15]. AA Alabduljabbar, J V Milanovic, "Assessment of techno-economic contribution of FACTS devices to power system operation", EPSR, 2010, Vol.80, pp:1247-1255
- [16]. Claudio A. Canizares, Antonio C. Z de Souza, and Victor H. Quintana, "Comparison of performance indices for detection of proximity to voltage collapse", Vol.11, No.3, August 1996, pp.1441-1450.
- [17]. A El Gallad, M.EI Hawary, "Particle swarm optimizer for Constrained Economic dispatch with Prohibited operating Zones", Proc. of IEEE conference, CCECE 2002, Vol.1, May 2002.
- [18]. P A Lof, T Smed, G Anderson, and D J Hill, "Fast calculation of a voltage stability index", IEEE Trans. on PS, Vol.7, No.1, February 1992, pp.54-64.
- [19]. Mota-Palomino R, Quintana V H. "Sparse reactive power scheduling by a penalty function linear programming technique", IEEE Trans Pwr Syst, 1986, Vol.1, No.3, pp.31-39.
- [20]. Alsac O, Stott B. "Optimal load flow with steady state security", IEEE Trans Pwr Appar Syst, 1974; PAS-93; pp.745-51.
- [21]. Yang H, Yang P, Huang C., "Evolutionary programming based economic dispatch for units with non-smooth fuel cost functions", IEEE Trans. Power Syst., 1996, Vol.11, pp:112-118.
- [22]. W. Ongsakul and T. Tantimaporn, "Optimal power flow by improved evolutionary programming", Electric Power Components and Systems, 2006, Vol.34, pp.79-95.
- [23]. Lin W, Cheng F, Tasy M., "An improved search for economic dispatch with multiple minima", IEEE Trans. Power Syst., 2002, Vol.17, pp.108-112.
- [24]. D Devaraj, B. Yegnanarayana., "Genetic Algorithm based optimal power flow for security enhancement", IEE Proc. on Gener. Trans. Distr., 2005, Vol.52, No.6, pp:899-905.